

# Complex $\gamma$ -ray Hologram: Solution to Twin Images Problem in Atomic Resolution Imaging

P. Korecki and G.Materlik

*Hamburger Synchrotronstrahlungslabor HASYLAB am Deutschen Elektronen-Synchrotron DESY, 22603 Hamburg, Germany*

J. Korecki

*Department of Solid State Physics, Faculty of Physics and Nuclear Techniques, University of Mining and Metallurgy,  
30-059 Kraków, Poland*

(October 27, 2000)

A new technique for high fidelity, artifact-free imaging of three-dimensional (3D) atomic structure with  $\gamma$ -ray holography is proposed and demonstrated experimentally. In this method two holograms are symmetrically recorded for both sides of the  $^{57}\text{Fe}$  Mössbauer resonance. Such detuning from the exact resonance condition produces a change in the phase of the nuclear scattering amplitude equal for all the scattering nuclei. By exploiting the linearity of the holographic pattern, it was possible to create two linear superpositions of the recorded holograms with corresponding nuclear scattering amplitudes differing in the phase by  $\pi/2$ , from which a new complex hologram was formed. The numerical holographic reconstruction was applied to this complex hologram resulting in a twin-image free 3D real-space image of the bcc Fe local structure. The proposed procedure allows the complete removal of the twin-images for an arbitrary position in real-space making  $\gamma$ -ray holography an unambiguous tool for atomic and magnetic structure imaging.

Internal source holography (ISH) [1] was proposed as a tool for three-dimensional model-free imaging of atomic structure. ISH employs the fact that the interference pattern formed by radiation emitted from a localized source inside a sample (atom or ensemble of equivalent atoms) can be interpreted as a hologram of the local atomic structure. ISH was introduced in electron diffraction [2] and subsequently applied in X-ray Fluorescence [3] and Bremsstrahlung [4] experiments. Also the time-reversed version of ISH was experimentally demonstrated for X-rays [5] and  $\gamma$ -rays [6]. Holographic methods are not limited to systems with a long-range order but can also be applied to clusters, surface adsorbates and impurities [7].

In the first step of such holographic procedure, an interference pattern:

$$I = |R + \sum_i O_i|^2 = R^2 + 2\text{Re} \sum_i R^* O_i + \dots \quad (1)$$

of waves  $O_i$  scattered by the object and a coherent reference wave  $R$  is recorded. If the object's waves are small ( $|\sum_i O_i| \ll |R|$ ) a three-dimensional image of the object can be reconstructed from the measured pattern in the second step, by illuminating this pattern with the reference wave alone [8]. As seen from Eq. (1) only the real part of the complex interference term (hologram) may be recorded, which results in the presence of twin-images (conjugate images) in real-space reconstruction of the object. For ISH real and twin-images occupy the same region in space distorting the reconstructed image. Very recently, for optical holography, it was demonstrated that twin-images can be eliminated by reconstructing a complex hologram which contains information about both the real and imaginary parts of the scattered waves [9].

In the time-reversed  $\gamma$ -ray holography [6] a sample containing a Mössbauer isotope ( $^{57}\text{Fe}$ ) is illuminated by radiation from a radioactive source ( $^{57}\text{Co}$ ). The incident photons can be directly absorbed in a recoilless, resonant process (holographic reference wave) or they can be additionally resonantly scattered on other nuclei (object waves). The intensity of the resulting interference field is probed at nuclear sites by measuring the conversion electron yield as the illumination direction is varied. The two-dimensional pattern (hologram) is then numerically reconstructed to real-space with a Fourier-like transform [10]. The  $\gamma$ -ray holography has several advantages when compared with x-ray holography. The nuclear scattering cross section value is high and the observed modulation of the total signal is several percent of the total signal which results in reasonable acquisition times even for a table-top experiment with a natural radioactive source. On the other hand, the cross section value is still low enough to insure that the object waves are much weaker than the reference wave and holographic reconstruction is possible. The most promising feature of  $\gamma$ -ray holography is the imaging possibility of a three-dimensional magnetic structure, similarly as in theoretically predicted method of spin electron holography [11] but without of any drawbacks connected with sophisticated nature of low-energy electron scattering. It could be performed by tuning to specific Mössbauer transition between the

sublevels split in the internal magnetic field specific for a crystal site. It has been suggested previously [12] that a model experiment demonstrating the magnetic resolution of  $\gamma$ -ray holography could be performed for magnetite in which Fe ions occupy two different crystallographic positions and the magnetic hyperfine fields at both sites differ enough to resolve site specific holograms.

Unfortunately, this possibility has not yet been realized. The main reason for this is just the presence of holographic twin-images. For particular systems, the real and twin images overlap and for a certain combination of interatomic distances and incident radiation energy they can sum up to zero, completely removing the information about particular scatterers from the reconstructed real-space image [13]. This difficulty may be overcome in electron holography and Multiple Energy X-ray Holography (MEXH) by collecting holograms for many wavelengths [14]. This method cannot be applied in the  $\gamma$ -ray holographic Mössbauer experiment where only a single wavelength is accessible.

As shown in Ref [12], the twin-image problem may be attacked directly by changing the phase of the nuclear scattering amplitude by detuning from the resonance, in a way similar to the X-ray anomalous diffraction techniques [15]. However, the numerical simulation showed that only a phase change of nearly  $\pi/2$  might solve this problem satisfactorily, nonetheless, it is not feasible to directly achieve such a big phase difference in a real experiment due to the rapid decrease of the scattering cross section far from the resonance. In the present study we propose a new idea of how to obtain the exact  $\pi/2$  phase shift and we demonstrate this possibility experimentally. We show a high fidelity 3D real-space reconstruction of the bcc-Fe structure, completely free of twin-images, obtained from a complex hologram, which had been constructed from the experimental holograms. In addition, presented results link the anomalous X-ray diffraction methods with the idea of complex holography.

The small size of the nucleus as compared to the radiation with a X-ray wavelength and a relatively simple polarization dependence of nuclear scattering, allow us to write the holographic formula for a single scattering nucleus as [12]:

$$\chi_1(\mathbf{k}, \Delta E) = \text{Re} \left[ \frac{f(\Delta E)}{r} e^{i(kr + \mathbf{k} \cdot \mathbf{r})} \right] \quad (2)$$

Equation (2) describes only the interference term between the reference wave, traveling from the  $\gamma$ -ray source placed far from the sample to an absorbing nucleus (the reference nucleus) located inside the sample at the origin, and an object wave additionally scattered by a single nucleus placed at position  $\mathbf{r}$ . In Eq. (2)  $\mathbf{k}$  is the wave-vector of the incident plane wave and the exponential factor resulting from the optical path differences. In the nuclear resonant scattering amplitude  $f(\Delta E) = |f(\Delta E)| e^{i\phi(\Delta E)}$  only the dependence on the energetic shift  $\Delta E$  from exact nuclear resonance, which has the width of the order of  $10^{-9}$  eV, is shown explicitly. This parameter may be easily tuned by changing the constant value of the Doppler velocity of the  $\gamma$ -ray source moved by a Mössbauer transducer. A more accurate expression for the  $\gamma$ -ray hologram, including the vectorial nature of the scattered waves, may be found in Ref. [12] or in Ref. [16], where it was derived in a rigorous quantum-mechanical approach. For monochromatic radiation or radiation with a Lorenz-like energy spectrum,  $f(\Delta E)$  has following properties characteristic for resonance scattering [17]:  $\text{Re}f(\Delta E) = -\text{Re}f(-\Delta E)$ ,  $\text{Im}f(\Delta E) = \text{Im}f(-\Delta E)$  and  $\phi(\Delta E = 0) = -\pi/2$ .

The twin-real image problem may be demonstrated considering the simplest centro-symmetric system consisting of a reference nucleus placed at the origin and two scattering nuclei at positions  $\mathbf{r}$  and  $-\mathbf{r}$ . Then, the corresponding hologram function may be written as:

$$\chi_2(\mathbf{k}, \Delta E) = 2|f(\Delta E)| \cos[kr + \phi(\Delta E)] \cos(\mathbf{k} \cdot \mathbf{r})/r \quad (3)$$

The real-space image function obtained from such hologram by applying the Fourier-like holographic transform [10] may be expressed as:

$$U(\mathbf{R}) = \int_S \chi(\mathbf{k}, \Delta E) e^{i\mathbf{k} \cdot \mathbf{R}} d\sigma_k \propto \cos[kr + \phi(\Delta E)] [j_0(k|\mathbf{R} - \mathbf{r}|) + j_0(k|\mathbf{R} + \mathbf{r}|)]/r \quad (4)$$

where the spherical Bessel functions  $j_0$  are simply the real or twin image of a point scatterer. It is apparent that the hologram and the reconstruction image are blind with respect to nuclear pairs for some values of the  $kr$  product, for which the cosine value reaches zero. It is also visible that this condition varies for different values of the scattering phase shift.

Consider first, a situation of scattering with pure imaginary or pure real scattering amplitude ( $\phi = -\pi/2$  or  $\phi = 0$ ). Hereafter, the corresponding holograms will be called real and imaginary holograms, respectively. In Fig. 1(a) calculated holograms of a single nucleus are shown for both cases. The real-space image functions reconstructed from both holograms are shown in Fig. 1(b) as a function of the distance between the imaged nuclear pair and the

reference nucleus. It is visible that both dependencies are exactly in anti-phase, which means that the twin-images can be removed by measuring both a real and an imaginary hologram. Imaginary holograms have already been recorded experimentally [6]. Unfortunately, it is not possible to directly record a real  $\gamma$ -ray hologram because the scattering amplitude is real only far from the resonance where the nuclear scattering cross section is negligible.

A hologram is a linear diffraction pattern. It is a linear function of the scattering amplitude unlike a conventional diffraction pattern recorded in the far-field containing its squared values. Furthermore,  $\gamma$ -ray holograms recorded close to the Mössbauer resonance correspond to the same wavelength since the relative energy change has a value of only (about)  $10^{-13}$ . Consider therefore a superposition of holograms recorded symmetrically for both sides of the Mössbauer resonance:

$$\chi_{\pm}(\mathbf{k}, |\Delta E|) = \chi_1(\mathbf{k}, +|\Delta E|) \pm \chi_1(\mathbf{k}, -|\Delta E|) \quad (5)$$

Using the properties of the nuclear scattering amplitude described above, it can be shown that:

$$\chi_{\pm}(\mathbf{k}, |\Delta E|) = \begin{cases} -2\text{Im}[f(|\Delta E|)] \sin(kr + \mathbf{k} \cdot \mathbf{r})/r \\ 2\text{Re}[f(|\Delta E|)] \cos(kr + \mathbf{k} \cdot \mathbf{r})/r \end{cases} \quad (6)$$

which is an important result for the purpose of this study. The linear superpositions from Eq. (5) of the holograms recorded symmetrically on both sides of the resonance are also holograms. Moreover, the resulting holograms are equivalent to real and imaginary holograms independent of the  $\Delta E$  parameter. The relative intensity of the holograms is given by a factor  $c = \text{Im}f(\Delta E)/\text{Re}f(\Delta E)$  for which the value of the order of 2 can be obtained even close to the resonance.

To show that the proposed procedure can be realized experimentally we performed a holographic experiment in a setup similar to the one described in Ref. [6], based on a conversion electron Mössbauer spectrometer. For practical experiment reasons, two  $\gamma$ -ray holograms of  $^{57}\text{Fe}(001)/\text{MgO}(001)$  epitaxial film were recorded with a  $^{57}\text{Co}$  source on the left side of the  $\frac{1}{2} \rightarrow \frac{3}{2}$  Mössbauer transition and on the right side of the  $-\frac{1}{2} \rightarrow -\frac{3}{2}$  transition (both lines give identical holograms in the resonance). The holograms were recorded symmetrically with respect to resonance with their effective energetic separation ( $2\Delta E$ ) being equal to the experimental FWHM of the Mössbauer line i.e. only a double decrease of the total number of counts with respect to the resonance detection was present. The corresponding asymmetry factor had a value of  $c = 2$  which allowed the construction of the linear superposition from Eq. (6) with a good signal-to-noise ratio.

Figure 2(a) shows linear superpositions of the recorded holograms. A slow varying background coming from the reference wave was subtracted and the holograms were symmetrized by operations corresponding to the 4-fold symmetry characteristic for the bcc structure of  $\alpha$ -Fe. To enhance the signal coming from the nearest nuclei a low-pass Fourier filter was applied to the images. For the following real-space transformation this filter was omitted. For comparison, real and imaginary holograms calculated according to Eq. (2) for two coordination shells around the absorbing nucleus are shown in Fig. 2(b). The agreement is good, confirming the possibility of obtaining holograms differing in the phase by  $\pi/2$  in an experiment.

Figure 3 shows real-space images obtained from the constructed experimental real and imaginary holograms expanded to a full reciprocal-space sphere in order to obtain isotropic spatial resolution [18]. The intensities of the nuclear images of the nearest ( $\frac{1}{2}\frac{1}{2}\frac{1}{2}$  positions in the unit cell) and the next-nearest neighbors (100 positions) are different for both real-space images as predicted by Eq. (4) and shown in Fig. 1 what is caused by the twin-images effect.

The twin-images will disappear for a hologram containing the whole information about the scattered waves i.e. about the real and imaginary part of the holographic interference term. The real and imaginary holograms from Eq. 6 can thus be combined to form a complex hologram:

$$h(\mathbf{k}, |\Delta E|) = \chi_+(\mathbf{k}, |\Delta E|) + ic\chi_-(\mathbf{k}, |\Delta E|) \quad (7)$$

which contains such information.

The real-space image of the bcc-Fe epitaxial film (consisting of islands with average diameter of 10nm) obtained from the complex hologram defined in Eq. (7) is presented in Fig. 4. The nuclei in the two coordination spheres are well imaged with an isotropic resolution of  $0.5\text{\AA}$  and with an experimental error in positions of about  $0.1\text{\AA}$ . Further nuclei are not imaged because of the divergence of the  $\gamma$ -ray beam and corresponding experimental angular resolution, which is a simple consequence of the sampling theorem. The intensities of the nuclear images in two coordination shells of 3D real-space are almost equal, proving that the cancellation of real and twin images is eliminated.

The presented procedure is very much different from the multiple-energy holographic algorithm [14]. Only two holograms are needed for the complete removal of the twin-images, whereas in the multiple-energy scheme an infinite

(high) number of holograms is needed. This result indicates practical possibility of using  $\gamma$ -ray holography to study the geometrical and especially the magnetic atomic structure of thin films and multilayers containing  $^{57}\text{Fe}$ . Holographic diffraction using  $\gamma$ -rays seems to be well suited for an investigation of those kind of systems, since the high divergence of the beam from radioactive sources fits very well with the slow angular variation of the holographic signals. Systems of interest do not need to have either long-range nor chemical order. In addition, for symmetrical detuning from the resonance, the mass absorption as well as the nuclear and electronic scattering cross sections are identical for  $\pm\Delta E$  and the related background will vanish for the difference hologram. Therefore, for a particular system, if the geometrical structure is known (and a pure real hologram is not blind to it) it will be possible to construct only the difference of the recorded diffraction patterns and the troublesome procedure of the background removal will be redundant. This will enable experiments on complex magnetic systems with a non-perfect structure and on magnetic nanostructures with low-concentration of the Mössbauer isotope (effectively only about 10 – 20 monolayers of  $^{57}\text{Fe}$ ), for which electronic scattering in the substrate is dominant and the time instabilities of the detection system can not be avoided due to long acquisition times.

- [1] A. Szöke, in *Short Wavelength Coherent Radiation: Generation and Application*, edited by D.T. Attwood and J. Bokor, AIP Conf. Proc. No. 147 (AIP, New York, 1986)
- [2] G. R. Harp, D. K. Saldin, B. P. Tonner, Phys. Rev. Lett. **65**, 1012 (1990)
- [3] M. Tegze and G. Faigel, Nature (London) **380**, 49-51 (1996).
- [4] S. G. Bompadre, T. W. Petersen, L. B. Sorensen, Phys. Rev. Lett **83**, 2741 (1999).
- [5] T. Gog et al., Phys. Rev. Lett. **76**, 3132 (1996)
- [6] P. Korecki, J. Korecki, and T. Ślezak, Phys. Rev. Lett. **79**, 3518 (1997)
- [7] C. M. Wei et al., Phys. Rev. Lett. **72**, 2434, (1994); K. Hayashi et al., Anal. Sci. **14**, 987 (1998)
- [8] D. Gabor, Nature (London), **161** 777 (1948)
- [9] S.-G. Kim, B. Lee, E.-S. Kim, Appl. Opt. **36** 4784, (1997); T.-C. Poon et al., Opt. Lett., **25** 215 (2000)
- [10] J. J. Barton, Phys. Rev. Lett. **61**, 1356 (1988)
- [11] E. M. E. Timmermans et al., Phys. Rev. Lett. **72** 832 (1994)
- [12] P. Korecki, J. Korecki, and W. Karaś, Phys. Rev. **B59**, 6141 (1999)
- [13] P. M. Len et al., Phys. Rev. **B50**, 11275 (1994)
- [14] J. J. Barton, Phys. Rev. Lett **67**, 3106 (1991)
- [15] *Resonant Anomalous X-Ray Scattering*, edited by G. Materlik, C. J. Sparks, and K. Fischer (North-Holland, Amsterdam, 1994)
- [16] J. Odeurs, R. Coussement, C. L'abbe, Phys. Rev **60** (1999)
- [17] G. T. Trammel, Phys. Rev. **126**, 1054 (1962)
- [18] M. Tegze et al., Phys. Rev. Lett. **82**, 4847 (1999)

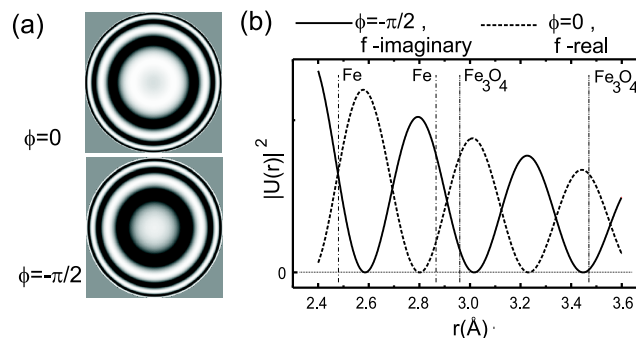


FIG. 1. (a) Calculated real and imaginary  $\gamma$ -ray holograms of a single nucleus. (b) Illustration of the real-twin images cancellation. Real space image function reconstructed from holograms of two nuclei placed symmetrically in respect to the absorbing nucleus shown as a function of the distance between the absorbing and scattering nuclei. The solid line represents the real space image function obtained from an imaginary hologram and the dashed line an image from a real hologram. The vertical lines mark the position of nearest Fe nuclei in bcc Fe and in magnetite, showing that for the latter the real-twin images cancellation is severe

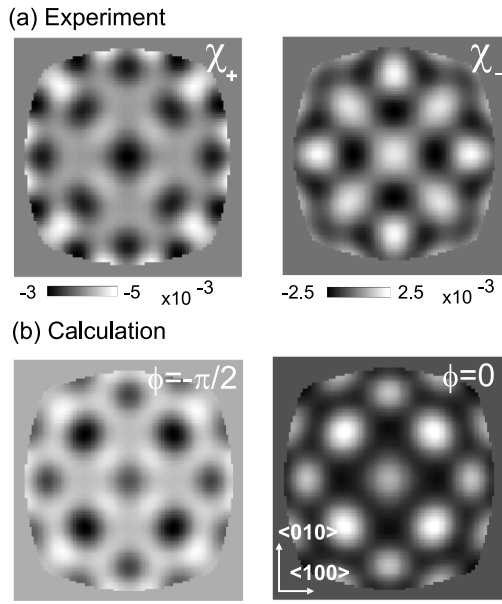


FIG. 2. (a) Holograms of bcc Fe local structure in an epitaxial Fe(001) film obtained by linear superpositions (sum and difference ) of two holograms recorded in experiment on opposite sites of the Mossbauer resonance. The gray intensity scale refers to the total signal and is of the order of  $5 \times 10^{-3}$  (b) Calculated real and imaginary holograms of nuclei in two coordination shells around the absorbing nuclei.

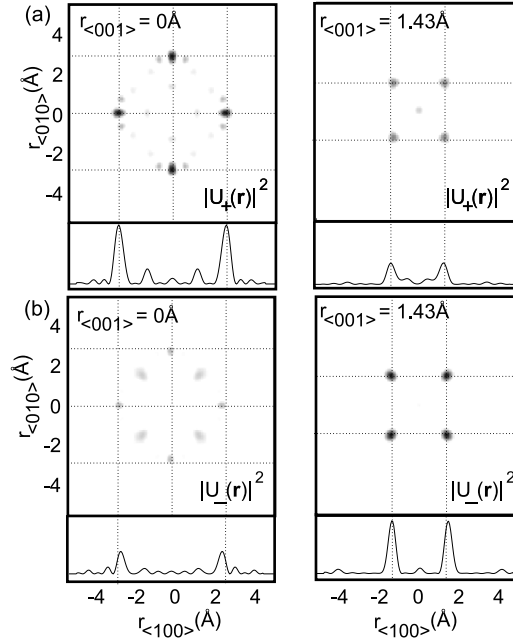


FIG. 3. Real-space images reconstructed from a sum (a) and a difference (b) of experimental holograms recorded for opposite sites of the Mössbauer resonance. For two-dimensional cuts, a linear gray scale is used. Cuts are presented for the plane containing the absorbing nucleus and 1.43Å above it. The one-dimensional profiles are drawn through the visible nuclear images.

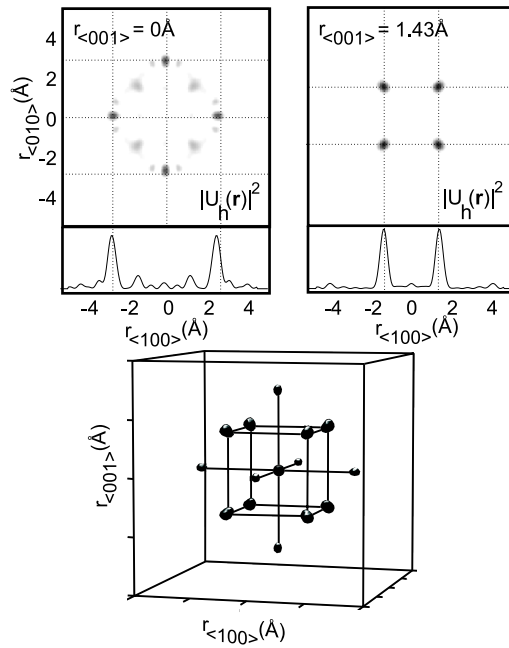


FIG. 4. Real-space images reconstructed from a constructed complex hologram. Cuts are presented for the plane containing the absorbing nucleus and  $1.43\text{\AA}$  above it. The one-dimensional profiles are drawn through the visible nuclear images. The 3D image is presented in a form of an isosurface at 40% of the maximum value of the whole real space image. The sphere in origin represents the absorbing reference nucleus. The sticks have a length equal to the lattice constant of bcc Fe